Slope Stability Using Non-Linear Failure Strength Criterion

N.K.Samadhiya
P.N.V.Mahesh Babu

Department of Civil Engineering
Indian Institute of Technology Roorkee
Roorkee – 247 667, India
Phone: +90-01332-285467(O); 285052 (R)
Fax: 01332 - 273560
Email: nksamfce@iitr.ernet.in

ABSTRACT

In the past, most of the slope stability analyses have been based on the linear Mohr-Coulomb failure strength criterion. The strength parameters c and ϕ are treated constant over the entire range of normal stresses. But actually, strength envelopes of almost all of the geomaterials are not linear. Therefore for rocks/soils c and ϕ values cannot be treated constant along the entire failure plane. With the nonlinear failure strength criterion, strength parameters c and ϕ may be considered according to the actual normal stresses. This paper presents analysis by limiting equilibrium method considering non-linear failure strength criterion, non-vertical slices and non-circular failure surface and interslice forces between slices. Non-linear failure strength criterion has been simplified as a linear, by taking tangents at each normal stresses. A computer program SANL.C developed in C^{++} language for the purpose has been used for the stability analysis.

Keywords: Slope stability analysis, non-linear failure criterion,

1. INTRODUCTION

For analysis of slopes, numerous methods are available. These methods differ in handling the degree of indeterminacy of the problem, shape of slip surface and slices. It becomes essential to consider non-circular slip surface and non-vertical & non-parallel slices, due to the structural weak planes existing in the sliding mass. Singh et al. (1996) have presented the analysis for the stability of slope with non-circular slip surface and non-vertical slices using linear strength criterion.

Yang et al. (2004) presented the limit analysis for stability of slope using non-linear failure strength criterion. They used method of generalized tangential technique. This method employs the tangential (a linear Mohr-Coulomb failure criterion), instead of the

actual non-linear failure criterion to formulate the work and energy dissipation and also to calculate stability factors.

In this paper, limiting equilibrium analysis has been developed for the stability of slopes using non-linear failure strength criterion, non-circular failure surface and non-vertical & non-parallel slices. The non-linear failure strength criterion is simplified as Mohr-Coulomb linear, by a set of straight lines, tangential to the non-linear failure strength criterion.

2. NON-LINEAR FAILURE STRENGTH CRITERION

In general, non-linear failure strength criterion is expressed as (Zhang and Chen, 1987; Drescher and Christopoulos, 1988)

$$\tau = c_0 \left(1 + \frac{\sigma_n'}{\sigma_t} \right)^{1/m} \tag{1}$$

where σ_n' and τ are normal and shear stresses on the failure surface, respectively. The values of c_0, σ_t and m are determined by laboratory tests. When m=1, Eq. (1) reduces to the well-known linear Mohr-Coulomb (MC) failure criterion. Hoek and Brown (1982) and Singh and Goel (2002) have suggested values of c_0 and m for rockmasses for different rock mass ratings.

The tangential line to the curve at the location of tangency point M as shown in Fig.1 is expressed as

$$\tau = c_t + \sigma_n \tan \phi_t \tag{2}$$

where ϕ_t = tangential frictional angle; c_t = intercept of the straight line on the τ-σ_n axis; σ_n = normal stress; and τ = shear stress. The c_t and ϕ_t at point M are determined by following expressions:

$$\tan \phi_t = \frac{d\tau}{d\sigma_n} = \frac{1}{m\sigma_t} c_0 \left(1 + \frac{\sigma_M}{\sigma_t} \right)^{(1-m)/m} \tag{3}$$

$$c_t = \frac{m-1}{m} c_0 \left(\frac{m\sigma_t \tan \phi_t}{c_0} \right)^{1/(1-m)} + \sigma_t \tan \phi_t \tag{4}$$

In Eq. (3), the stress σ_M is the value of normal stress at the tangency point M as shown in Fig. 1. In order to ensure that the tangential line always lies outside of the curve, and that the strength corresponding to the tangential line is more than or equal to that of the corresponding non-linear curve, the requirement $m > 1$ is to be satisfied.

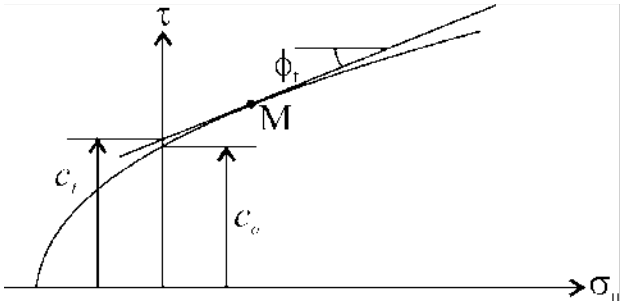

Fig. 1 - Tangential line for a non-linear failure criterion
(Yang et al., 2004)

The generalized tangential technique uses a nonlinear failure criterion in Eq. (1) as a linear MC failure criterion in Eq. (2) with a tangential line to the non-linear failure criterion.

3. FORMULATION FOR PROPOSED METHOD OF STABILITY ANALYSIS

The method advocated here is based upon the physical requirement that sliding on a polygonal surface is only possible kinematically if a sufficient number of internal shear surfaces can develop. The sliding mass is divided into slices and then equations of statics are applied to each slice and the factor of safety and other useful parameters are obtained.

3.1 Assumptions

The following assumptions are made in the method being presented here.

(a) The approach of limit equilibrium can be applied to slopes satisfactorily.
(b) The blocks comprising the slope mass are rigid, and only sliding but no rotation or lifting-off of the potential sliding mass occurs.
(c) Sufficient numbers of internal slip surfaces are present and their directions are known.
(d) On the internal and external sliding surfaces (at the condition of limit equilibrium) the Mohr-Coulomb failure condition is applicable. The strength parameters may be allocated different values on each sliding surface.
(e) The same value of factor of safety is assumed for the internal and external sliding surfaces.
(f) Cohesion and angle of internal friction are calculated for each slice depending upon the nonlinear coefficient.
(g) Nonlinear coefficient should be always greater than one.

3.2 Factor of Safety and Interslice Forces

The potential sliding mass is divided into n slices. Thus there are total n slices and (n+1) sides. Out of these n slices, the i^{th} slice is considered for the analysis. The various forces acting on i^{th} slice are shown in Fig. 2. The notations are as follows.

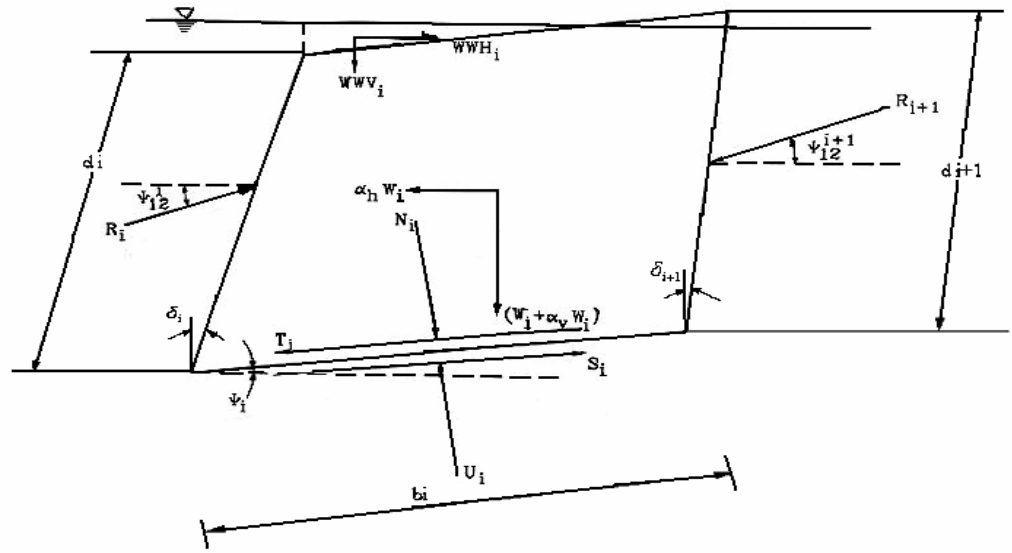

Fig. 2 - Definition of various forces acting on the i[th] slice (Shekhawat, 1993)

W_i = weight of i[th] slice,

α_h = coefficient of horizontal earthquake acceleration,

α_v = coefficient of vertical earthquake acceleration,

N_i = total normal force on the base of slice,

U_i = total pore water pressure on the base of slice

= $u_i b_i$

S_i = shear resistance on the base of slice

T_i = shear force on the base of slice,

WWV_i = vertical force due to water above the top of the slice,

WWH_i = horizontal force due to water above the top of slice,

R_i = interslice force on side i,

R_{i+1} = interslice force on side $i+1$,

$\psi_{12}^{\ i}$ = angle of R_i from horizontal,

$\psi_{12}^{\ i+1}$ = angle of R_{i+1} from horizontal,

b_i = width of the base of slice,

d_i = length of slice i,

d_{i+1} = length of slice *(i+1)*,

δ_i = inclination of side i from vertical,

δ_{i+1} = inclination of side *(i+1)* from vertical, and

ψ_i = dip (inclination with horizontal) of the base of slice.

Resolving the forces along the normal to the base of slice.

$$N_i = [W_i + \alpha_v W_i]\cos\psi_i - \alpha_h W_i \sin\psi_i + R_i \sin\left[\psi_i - \psi_{12}{}^{i}\right] - R_{i+1}\sin\left[\psi_i - \psi_{12}{}^{i+1}\right] + WWV_i \cos\psi_i + WWH_i \sin\psi_i \quad (5)$$

$\therefore$ Effective normal force on base,

$$\begin{aligned} N'_i &= N_i - U_i \\ &= N_i - u_i b_i \\ &= [W_i + \alpha_v W_i]\cos\psi_i - \alpha_h W_i \sin\psi_i + R_i \sin\left[\psi_i - \psi_{12}{}^{i}\right] \\ &\quad - R_{i+1}\sin\left[\psi_i - \psi_{12}{}^{i+1}\right] + WWV_i \cos\psi_i + WWH_i \sin\psi_i - u_i b_i \end{aligned} \quad (6)$$

Resolving along the base of the slice,

$$\begin{aligned} T_i &= [W_i + \alpha_v W_i]\sin\psi_i - \alpha_h W_i \cos\psi_i - R_i \cos\left[\psi_i - \psi_{12}{}^{i}\right] \\ &\quad + R_{i+1}\cos\left[\psi_i - \psi_{12}{}^{i+1}\right] + WWV_i \sin\psi_i - WWH_i \cos\psi_i \end{aligned} \quad (7)$$

$$S_i = N'_i \tan\phi_i + b_i c_{ti} \quad (8)$$

where

c_{ti} = cohesion for the base of slice i, and

ϕ_{ti} = friction angle for the base of slice i.

$\therefore$ Factor of safety, $F_i = \dfrac{S_i}{T_i}$ (9)

And, overall factor of safety, $FS = \dfrac{\sum_1^n S_i}{\sum_1^n T_i}$ (10)

Let $F_i = FS, \quad i = n, n-1, \ldots\ldots\ldots\ldots 2,1$

Then, from Eq.(10),

$$FS.T_i = S_i$$

Making use of Eqs.(7) and (8),

$$\begin{aligned} &FS\left[\begin{aligned}&(W_i + \alpha_v W_i)\sin\psi_i + \alpha_h W_i \cos\psi_i - R_i \cos\left(\psi_i - \psi_{12}{}^{i}\right) + R_{i+1}\cos\left(\psi_i - \psi_{12}{}^{i+1}\right)\\ &+ WWV_i \sin\psi_i - WWH_i \cos\psi_i\end{aligned}\right] \\ &= b_i c_{ti} + \tan\phi_{ti}\left[\begin{aligned}&(W_i + \alpha_v W_i)\cos\psi_i - \alpha_h W_i \sin\psi_i + R_i \sin\left(\psi_i - \psi_{12}{}^{i}\right)\\ &- R_{i+1}\sin\left(\psi_i - \psi_{12}{}^{i+1}\right) + WWV_i \cos\psi_i + WWH_i \sin\psi_i - u_i b_i\end{aligned}\right] \end{aligned}$$

If, $C_4 = \tan\phi_{ti}\sin\left[\psi_i - \psi_{12}{}^{i}\right] + FS.\cos\left[\psi_i - \psi_{12}{}^{i}\right]$ and

$$C_3 = FS\begin{bmatrix}(W_i + \alpha_v W_i)\sin\psi_i + \alpha_h W_i \cos\psi_i + R_{i+1}\cos\left(\psi_i - \psi_{12}{}^{i+1}\right)\\ + WWV_i \sin\psi_i - WWH_i \cos\psi_i\end{bmatrix}$$
$$- b_i c_{ti} - \tan\phi_{ti}\begin{bmatrix}(W_i + \alpha_v W_i)\cos\psi_i - \alpha_h W_i \sin\psi_i - R_{i+1}\sin\left(\psi_i - \psi_{12}{}^{i+1}\right)\\ + WWV_i \cos\psi_i + WWH_i \sin\psi_i - u_i b_i\end{bmatrix}$$

Then, $R_i = \dfrac{C_3}{C_4}$ (11)

3.3 Direction of Interslice Forces

Since, the limit equilibrium condition occurs at the sides also, so the angle of interslice force with the normal to the side is equal to ϕ_{mi}, i.e. mobilized angle of friction on sides. Value of ϕ_{mi} is given as

$$\tan\phi_{mi} = \frac{1}{\underline{F_i}}\left[\tan\phi_{si} + \frac{\underline{c_{si}}.\underline{A_i}}{R_i\cos\phi_{mi}}\right] \quad (12)$$

where,

$\underline{F_i} = F_i[1, R_i \sin\phi_{mi}]$,

$\underline{c_{ti}} = c_{si} - \dfrac{PW_i}{\underline{A_i}}\tan\phi_{si}$,

PW_i = water force on side i,

ϕ_{si} = friction angle in side i,

c_{si} = cohesion on side i,

F_i = factor of safety for wedge i,

$\underline{A_i}$ = area of side i,

= d_i (considering unit thickness),

sign (a_1, a_2) = function with magnitude a_1 and sign of a_2,

$R_i \sin\phi_{mi}$ = tangential component of R_i, and

$R_i \cos\phi_{mi}$ = normal component of R_i.

Since, Eq. 12 is an implicit equation, so initially $\underline{c_{si}}$ is taken as zero. The Eq.12 then reduces to

$$\tan\phi_{mi} = \frac{\tan\phi_{si}}{\underline{F_i}} \quad (13)$$

Using Eq.(13), ϕ_{mi} is obtained and is substituted in the right hand side of Eq. (12) and new value of ϕ_{mi} is obtained. The iterations on the value of ϕ_{mi} are done till the

convergence occurs. Once the value of ϕ_{mi} is known, the value of $\psi_{12}^{\ i}$ can be obtained as,

$$\psi_{12}^{\ i} = \phi_{mi} - \delta_i \tag{14}$$

3.4 Procedure of Calculation

The calculation for factor of safety and interslice forces is done in following steps.

Step 1: For each effective normal stress ($\sigma_n^{'}$), calculate tensile stress (σ_t), using the Eq (1) for each slice.
Step 2: Calculate c_t and ϕ_t for each slice, using nonlinear coefficient (m) from Eqs.3 and 4.
Step 3: Consider the overall equilibrium and calculate a value of factor of safety from Eq.10, assuming $R_i = 0$.
Step 4: Find the direction of interslice forces, as described in Art.(3.3).
Step 5: Consider nth slice at the top of the slope. Since value of Rn+1(water thrust in tension crack) is known, calculate R_n by making use of Eq.11.
Step 6: Consider next $(n-1)^{th}$ slice and calculate R_{n-1} successively, thus calculate all interslice forces. Please note that $R_1=0$ as first side of first wedge is free surface of slope.
Step 7: Now calculate factor of safety of each wedge by making use of Eq.9.
Step 8: Repeat the above steps (1) to (7), 2n times taking into account the values of interslice forces obtained in step (6). It is observed that in 2n cycles the convergence is achieved.
Step 9: Try another kinematically possible slip surface to obtain lowest factor of safety.

The above mentioned steps are performed by using the computer program SANL.C, which is described in further sections.

3.5 Dynamic Settlement and its Calculation

The analysis of the dynamic stability of slopes and embankments should be based on the dynamic displacement approach rather than the factor safety approach. During earthquake, the factor of safety may fall below unity several times (for very small fraction of second), but unless the dynamic displacement becomes considerable the slope should not be considered as unstable.

To calculate dynamic settlement correlation of Jansen (1990) has been used. First of all critical acceleration i.e. acceleration for unit factor of safety is calculated. It is based on the assumption that 1/F varies linearly with α_h. The dynamic displacement may be computed using Eq.15 as given below:

$$S_{dyn} = 5.8\ (0.1M)^8\ [(\alpha_h - \alpha_{cr})/(\alpha_{cr})]^{0.5} \tag{15}$$

where

S_{dyn} = dynamic settlement in metres,

M = magnitude of design earthquake on Richter scale, and

α_{cr} = critical coefficient of horizontal earthquake acceleration for dynamic factor of safety of 1.0.

The slope is considered to be unstable if dynamic settlement exceeds 0.01 times the slope height or 1m whichever is less.

4. DEVELOPMENT OF SOFTWARE PACKAGE (SANL.C)

The various equations derived in previous articles can be solved by several iterations only. Manually solving a number of equations iteratively is a time consuming and somewhat inaccurate way of handling the situation. Therefore computer program SANL.C has been developed in C^{++} language.

The input to the program consists of the geometry of slices, position of phreatic line, parameters representing non-linear strength criterion and unit weights of slope mass and water. The output gives nonlinear values of cohesion and internal friction for each slice, weight, pore water pressure, factor of safety (static and dynamic), critical acceleration, dynamic displacement, interslice forces. The program logic is described in the following sections.

The program SANL.C comprises of main program which calls subroutines INPUT, BL and SIDE. The flowchart for the main program is shown in Fig 4. The flow charts for subroutines are presented in Figs. 5 to 7. The subroutines are self explanatory.

5. USER'S MANUAL

The sequence of input data to be given in file, for the convenience of user and definitions of various parameters coming into picture in the program are being given.

5.1 Sequence of data in the input file

The various input data should be written in the input file in the sequence being given below.

N
AH AVR EQM GAMAW R (N1) M
XT(I) YT(I) XB(I) YB(I) XW(I) YW(I) CS(I) PHIS(I)
(For each slice side i.e. total N+ 1 line)
C (I) PHI (I) SIGMAT (I) GAMA (I)

(For base of each wedge, i.e. total N lines)

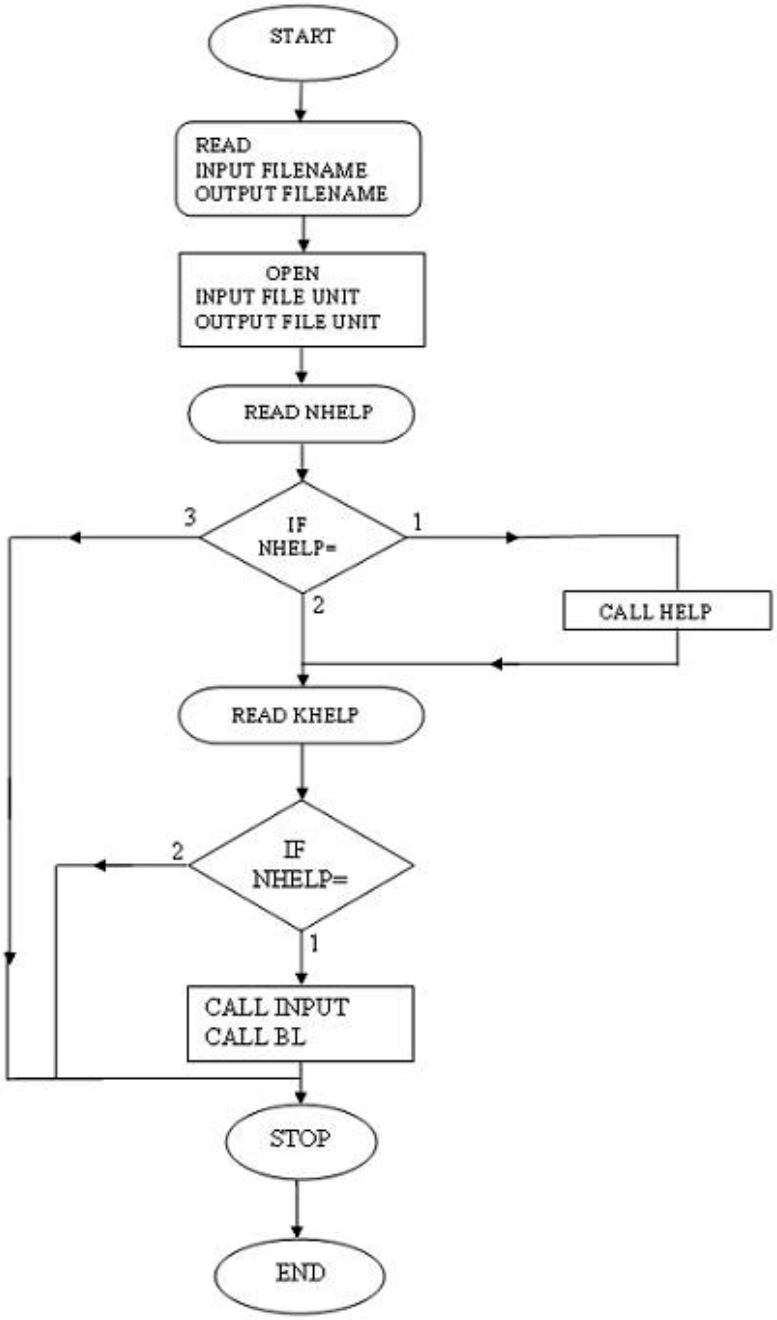

Fig. 3 - Flow chart for MAIN program

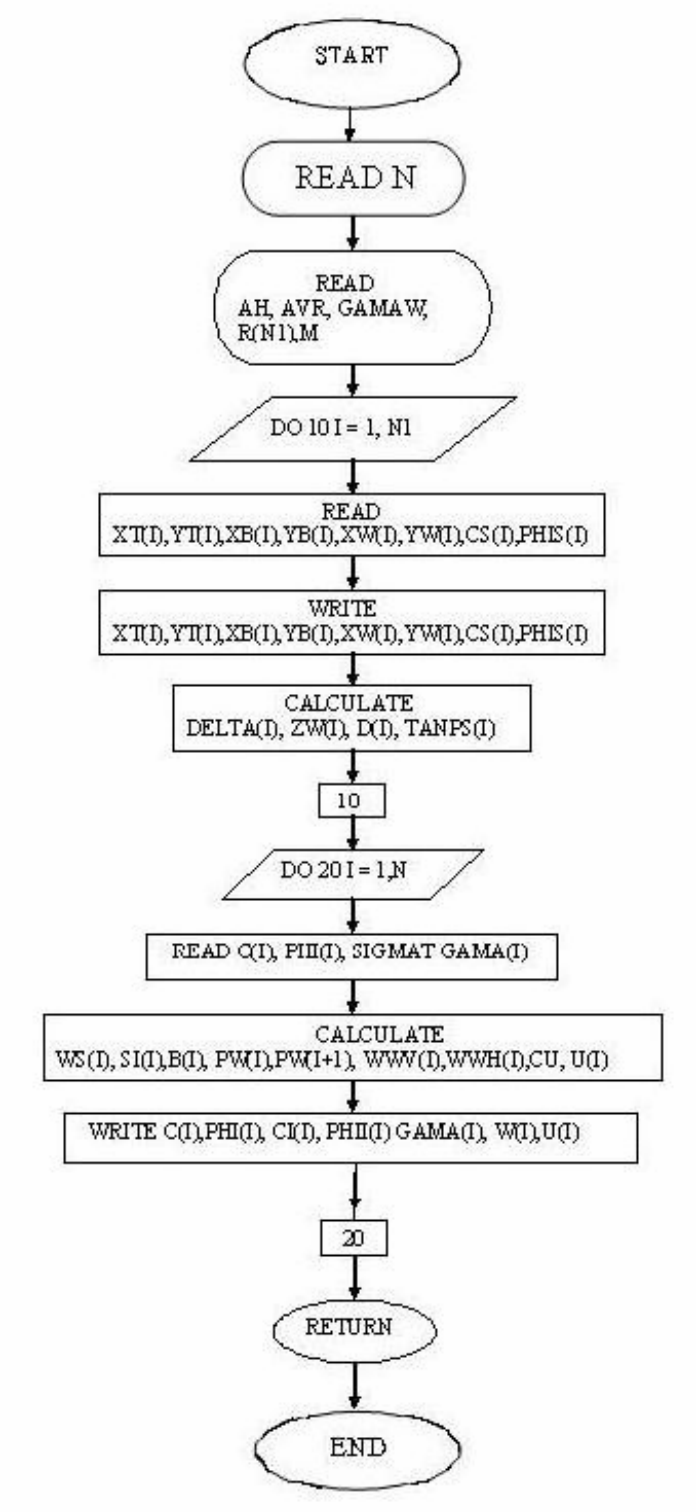

Fig. 4 - Flow chart for subroutine INPUT

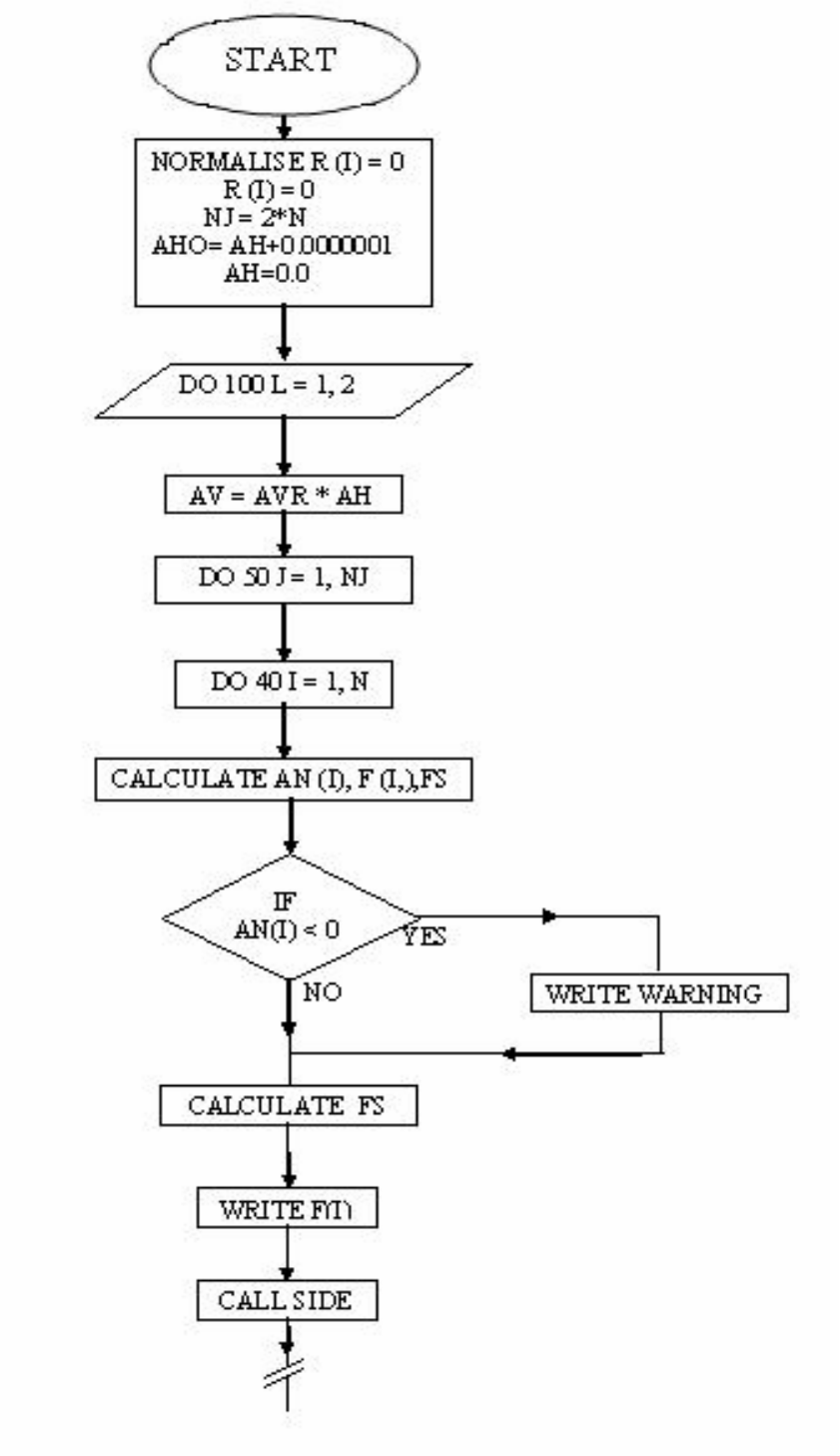
START
NORMALISE R (I) = 0
R (I) = 0
NJ = 2*N
AHO= AH+0.0000001
AH=0.0
DO 100 L = 1, 2
AV = AVR * AH
DO 50 J = 1, NJ
DO 40 I = 1, N
CALCULATE AN (I), F (I,),FS
IF
AN(I) < 0
YES
NO
WRITE WARNING
CALCULATE FS
WRITE F(I)
CALL SIDE

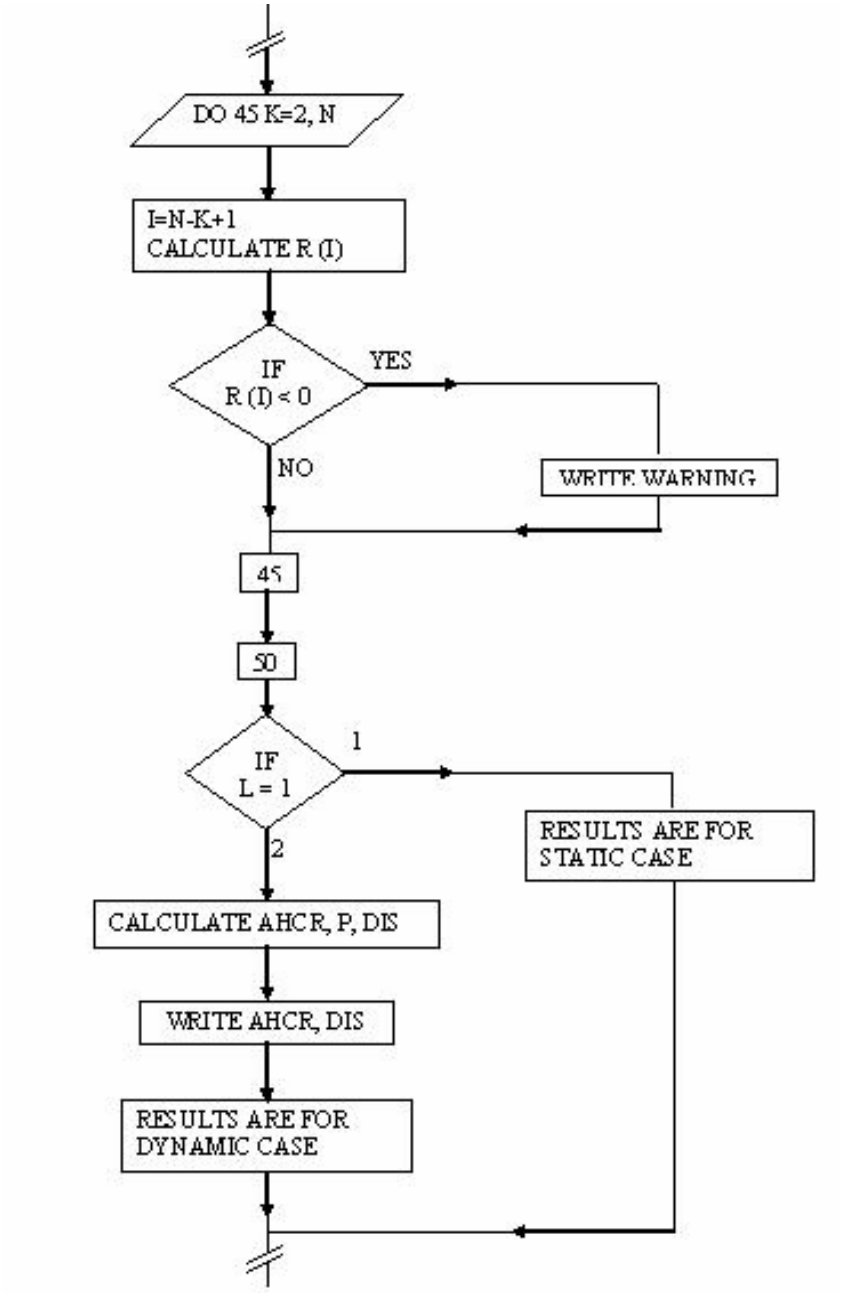
DO 45 K=2, N
I=N-K+1
CALCULATE R (I)
IF
R (I) < 0
YES
NO
WRITE WARNING
45
50
IF
L = 1
1
2
RESULTS ARE FOR
STATIC CASE
CALCULATE AHCR, P, DIS
WRITE AHCR, DIS
RESULTS ARE FOR
DYNAMIC CASE

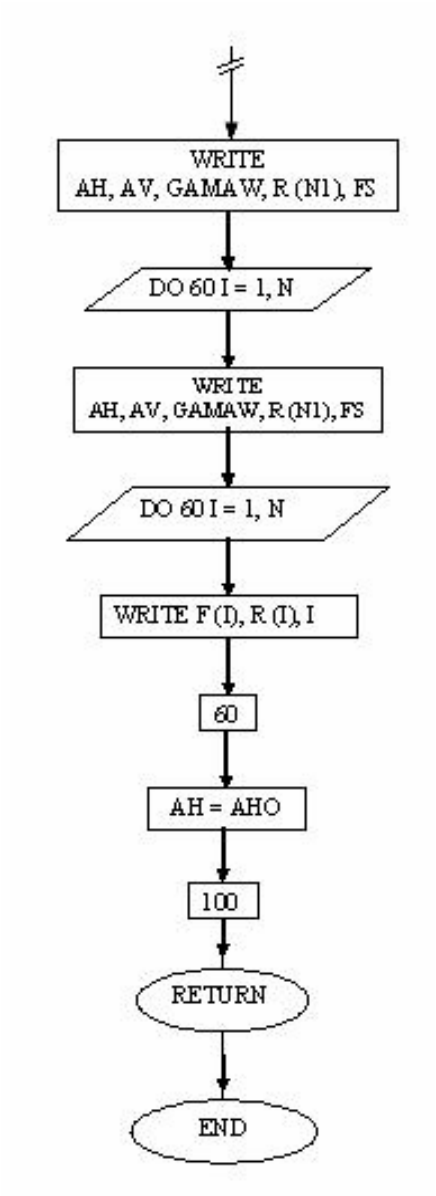

Fig. 5 - Flow chart for subroutine BL

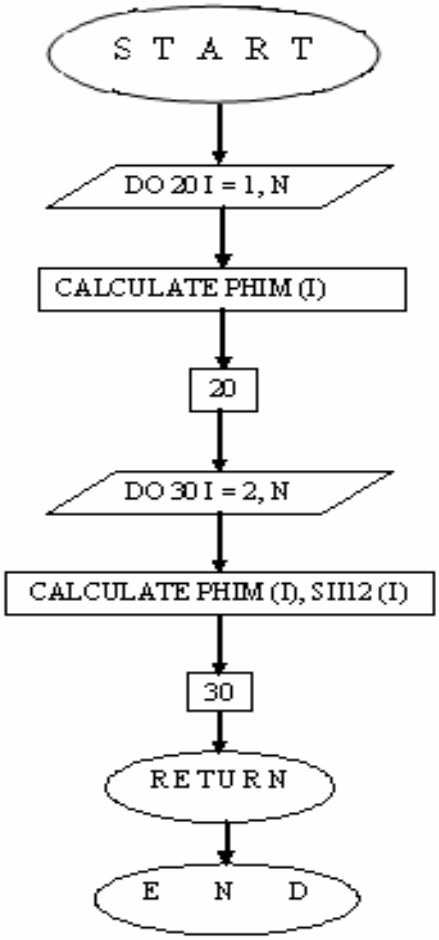

Fig. 6 - Flow chart for subroutine SIDE

5.2 Definitions of Various Parameters

AH	= coefficient of horizontal earthquake acceleration
AHCR	= critical acceleration i.e. acceleration corresponding to factor of safety equal to unity.
AV	= coefficient of vertical earthquake acceleration
AVR	= AV/AH
AN(I)	= normal force on the base of slice I
SIGMAT(I)	= tensile stress for each slice
B(I)	= base width of slice I
C(I)	= cohesion for the base of slice I
CS(I)	= cohesion for the slice side I
CI(I)	= cohesion at the base of slice after considering nonlinear coefficient
CU	= correction for area of base pore water pressure
DELTA(I)	= inclination of slice side I, from vertical
D(I)	= length of slice side I

DIS = dynamic displacement
F(I) = factor of safety for slice I
FS = overall factor of safety.
GAMA(I) = unit weight of material of slice I
GAMAW = unit weight of water
M = magnitude of earthquake on Richter's scale
N = total no. of slices
N1 = N+1
P = AHCR/AH
PW(I) = porewater pressure on side I
PHI = friction angel for base of slice(I) (in degrees)
PHIS(I) = friction angle for side I (in degrees)
PHIM(I) = mobilized friction angle on side I (in radians)
PHII(I) = friction angle for base of slice I after considering nonlinear coefficient (in degrees)
R(I) = interslice reaction on side I
SI(I) = dip of the base of slice I (in degrees)
SII12(I) = dip of the interwedge reaction R(I) (in radians)
U(I) = porewater pressure at the base of slice I
W(I) = weight of slice I (dry weight)
WWH(I) = horizontal component of water force, due to water above the top of slice I
WWV(I) = vertical component of water force, due to water above the top of slice I
XB(I) = x-coordinate of base of side
XW(I) = x-coordinate of phreatic surface on side I
XT(I) = x-coordinate of top of side I
YB(I) = y-coordinate of base of side I
YW(I) = y-coordinate of phreatic surface on side I
YT(I) = y-coordinate of top of side I
ZW(I) = YW(I)-YB(I)

6. CASE STUDIES

The developed program SANL.C was used to analyse several slopes to validate the program. The results of the linear analysis (m =1) compare excellently well with the results obtained from the computer program SANC.FOR (Shekhawat, 1993).
Four typical case studies from the available literature were chosen for further analysis and the results are presented as under.

6.1 Case Study 1

Shelbyville Dam (Hassan and Thomas, 2000)

The structure is located on the Kaskaskia River in central Illinois, USA, about 160km northeast of St.Louis, Missouri. The dam is a combined earth-fill and concrete gravity structure with a total length of 1,034m. Its maximum height is 33m and consists of a

homogeneous section with upstream and downstream berms, an inclined chimney drain and a horizontal drainage blanket. The embankment is constructed over a thin sand layer resting on a firm rock foundation. The main earth embankment cross section is shown in Fig 7. Failure surface and geometry of slices are shown in Fig .8.

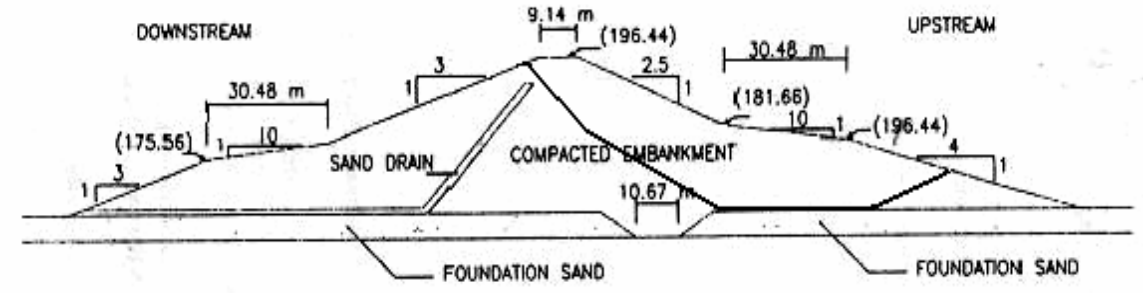

Fig. 7 - Cross-section of Shelbyville Dam (Hassan and Thomas, 2000)

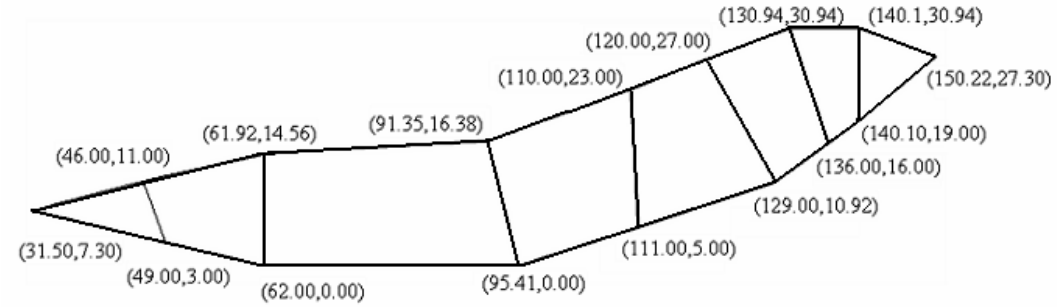

Fig. 8 - Geometry of slope 1

6.2 Case Study 2

A Landslide in Boulder Clay at Selset, Yorkshire (Skemmpton and Brown, 1961)

An analysis has been made in a valley slope of the River Lune, near Middleton-in-Teesdale. The slip was entirely within a deposit of heavily over-consolidated intact boulder clay. The slip is located in the south slope of the River Lune valley, 183m upstream of Selset. Bed-rock consisting of sandstone, shale, and limestone strata of the Lower Carboniferous, is found at a depth of about 9.14m beneath the valley floor. The rocks dip in a south-easterly direction at an angle of about 6°. They are overlain by massive deposits of heavily over-consolidated boulder clay which extend, up to an elevation of 304.8m. Analysis for critical failure surface is done and geometry of slices are shown in Fig. 9.

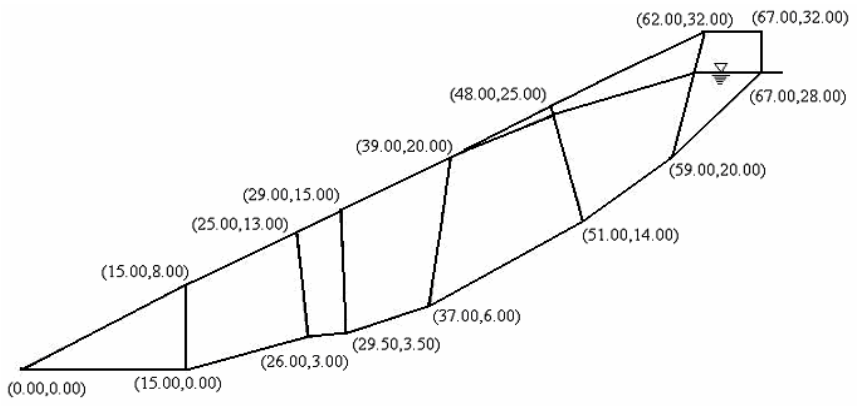

Fig. 9 - Geometry of slope 2

6.3 Case Study 3

Slope Failure in Phyllitic Clay (Sitaram et al., 1995)

Slope failure in Bicholim Mine (Dempo Mining Corporation Ltd., Goa), in Goa occurred in 1991. Analysis of slope failure done by Janbu's method, Spencer and Wright method (circular and non-circular failure surface) and Bishop's method. Slope strata consists of laterite, phyllitic clay, manganiferous clay etc. physical and mechanical properties of phyllitic clay are specific Gravity is 2.404, dry density 15.98kN/m^3, saturated density 19.15 kN/m^3, cohesion is 15.69 kN/m^2 and angle of internal friction is 22º. This slope is analysed by considering non-circular non-vertical slices and non-linear strength criterion and geometry of slope is shown in Fig.10.

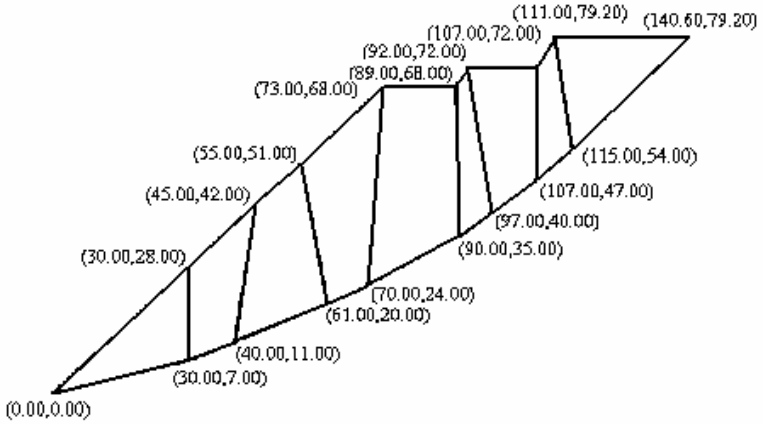

Fig. 10 - Geometry of slope 3

6.4 Case Study 4

Slope Design of the Maton Rock Phosphate Mine (Singh et al., 1997)

The Maton rock Phosphate Deposit is being mined by M/s Hindustan Zinc Ltd. The deposit is approximately 12km south east of Udaipur, Rajasthan. The mine is situated in

the semi-arid desert condition of Rajasthan. The maximum depth of the mine will be 120m and yearly ore production is 57,000tones. The objective was to determine the optimum (safe and steepest) slope angle in the footwall and hanging wall. Geotechnical mapping was done on the exposed benches of the slope. Slope strata consists of fractured quartzite. At places, small shear planes are also present. Along which quartzite has become a powdery material. Big boulders are embedded in soil mass. The samples of the rock and soil were tested for studying the physico-mechanical properties. For the slope mass unit weight is 19.32kN/m^3, angle of internal friction is 30º and cohesion is 76.52kPa. The overall slope height is 60m and ground water condition is 20m above the toe of the slope. The geometry of slope considered for analysis is shown in Fig.11.

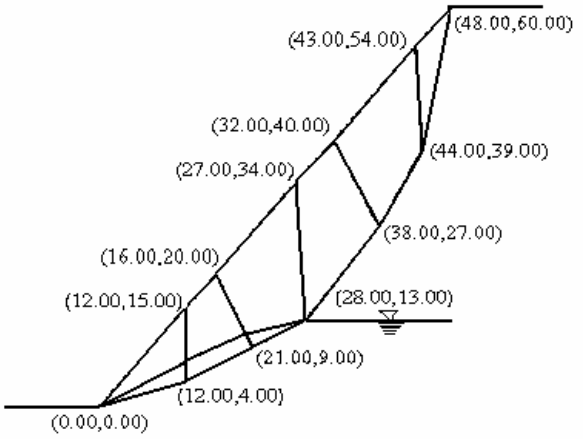

Fig. 11 - Geometry of slope 4

7. RESULTS AND DISCUSSION

Table 1 presented the results of the analysis carried out using SANL.C for the case studies described above.

Table 1 - Factor of safety based on the non-linear coefficient (*m*)

	m	1.0	1.20	1.40	1.60	1.80	2.00	2.50
Case Study,1	Factor of Safety	3.33	3.16	3.04	2.96	2.89	2.84	2.75
Case Study,2	Factor of Safety	0.87	0.64	0.49	0.41	0.36	0.32	0.26
Case Study,3	Factor of safety	0.83	0.56	0.42	0.34	0.29	0.26	0.21
Case Study,4	Factor of Safety	1.25	1.13	1.05	1.00	0.97	0.94	0.90

From Table 1, it is evident that by using non-linear failure strength criterion, factor of safety is found to be decreasing with non-linear coefficient m. Therefore, it is strongly recommended to use non-linear strength criterion, so that actual strength parameters operative during failure and not the average strength parameters are considered in the analysis.

8. CONCLUSIONS

By using non-linear failure strength criterion, factor of safety decreases. This is because of actual strength parameters operative during failure and not the average strength parameters are considered in the analysis. So, the non-linear failure strength criterion is strongly recommended. Proposed program SANL.C is easy to use for analyzing the complex landslides, non-homogeneous dams, talus/debris slides, planar rock slides and other types of failures of slopes in seismic area. Four case histories have been analysed

References

Drescher, A., and Christopoulos, C. (1988). Limit analysis slope stability with nonlinear yield condition, Int. J. Numer. Analyt. Meth. Geomec., 12(3), pp 341-345.

Hassan, M. Ahmed and Wolff, F. Thomas. (2000). Slope stability 2000, Proceedings of Sessions of Geo-Denver-2000, Geo-Institute of ASCE, August 5-8, Denver, Colorado, pp 194-208.

Jansen, R.B. (1990). Estimation of embankment dam settlement caused by earthquake, Water Power and Dam Construction, pp 35-40.

Shekhawat, R.K. (1993). Stability analysis of slopes with non-circular slip surface and non-vertical slice, M.E. Dissertation, Civil Engineering Department, University of Roorkee, Roorkee.

Singh, Bhawani and Goel, R.K. (2002). Software for engineering control of landslide and tunneling, A.A. Balkema, Table 6.1, pp 344.

Singh, Bhawani., Samadhiya, N.K. and Shekhawat, R.K. (1996). Stability analysis of slopes with non-circular slip surface and non-vertical slices, Indian Geotech.J. 26 (4), pp 417-429.

Singh, V.K., Singh, J.K. and Kumar, A. (1997). Slope design of the maton rock phosphate mine, Indian Geotechnical Conference, Vadodara, pp 585-588.

Sitaram, N., Narendar, K.R., and Venkateswarlu, V. (1995). Slope failure in phyllitic clay – a case study, Indian Geotech. Conference, Vol. 1. Bangalore, pp 271-273.

Skempton, A. W., and Brown, J.D. (1961). A land slide in boulder clay at seleset, Yorkshire, Geotechnique, 11, pp 28.-293.

Yang, Xiao-Li and Yin, Jian-Hua. (2004). Slope stability analysis with nonlinear failure criterion, Journal of Engg. Mechanics, Vol. 130, 3, pp 267-273.

Zhang, X.J. and Chen, W.F. (1987). Stability analysis of slopes with general nonlinear failure criterion, Int. J. Numer. Analyt. Meth. Geomech., 11(1), pp 33-50.

Hoek, E. and Brown, E.T. (1980). Underground excavations in rock, The Institute of Mining and Metalling, London, Table 12, p. 527.

Maheshbabu, P.N.V. (2005). Slope stability using non-linear failure strength criterion, M. Tech. Dissertation, Civil Engineering Department IIT Roorkee, p. 82.